H∞-based Position Control of a 2DOF Piezocantilever Using Magnetic Sensors.

Juan Antonio Escareno, Joël Abadie, Micky Rakotondrabe, Emmanuel Piat

H_∞-based Position Control of a 2DOF Piezocantilever Using Magnetic Sensors

J. Escareno[1], J. Abadie[2], M. Rakotondrabe[2], E. Piat[2]

***Abstract*— The article addresses the position control problem of a 2 degrees of freedom (DOF) piezoelectric cantilever by means of an embedded magnetic-based position sensor. The active part of the piezocantilever used in the experimental setup is similar to cantilevers previously developed and already used for low-frequency micro-actuators in microrobotics devices. The contribution relies on the estimation of the biaxial displacement of the piezocantilever via conventional Hall-effect (HE) sensors, reducing the mechanical complexity and cost aspects. The actual sensing approach is validated via the implementation of a real-time position control based on the H_∞ scheme. In comparison with high resolution sensors, as laser or confocal chromatic (high-cost) or capacitive displacement (bulky), the actual sensor-control system is provides a satisfactory performance to cope with traditional micro-positioning tasks requiring a micrometer resolution. The performance of the embedded magnetic-based position sensor is evaluated, in open- and closed-loop, with respect the measurements provided by a Keyence laser sensors.**

I. Introduction

Piezoelectric materials are well appreciated for the development of precise positioners. This recognition is mainly due to the high resolution, the high bandwidth and the high stiffness they can offer. Furthermore, the fact that they are powered electrically makes them easy to setup. Finally, their inherent property of physical reversibility makes them usable for sensors, or actuators or both (self-sensing). PZT materials (lead zirconate titanate) which are ceramics are the most used piezoelectric materials because they are widely available for a low cost, and their coupling coefficient is high relative to almost other piezoelectric materials. However, these materials are typified by nonlinearities (hysteresis and creep) that result in a loss of the overall accuracy of the positioners. Moreover, many structures of positioners (cantilever structures) yield badly damped oscillation at their response which may compromise their stability. To overcome these unwanted effects, different control techniques of the positioners have been proposed. While open-loop (feedforward) control techniques were able to reject the nonlinearities and to damp the oscillation with a high packageability level of the overall system [3][4][5][6][7][8][9], their main limitation is the lack of robustness face to model uncertainties or to external disturbance. Contrary to feedforward techniques, closed-loop control techniques (feedback) can offer better robustness by rejecting the effects of the above mentionned nonlinearities and oscillation. They also permit to reach substantial overall performances (accuracy, repeatability, external disturbance rejection). Different feedback techniques have been used: PID structures with simple tuning, passivity technique, robust H_∞ technique, robust interval techniques...[10][11][12][13]. However, feedback control of miniaturized piezoelectric based systems and positioners are limited to the lack of convenient sensors as we will detail in the next paragraph. In addition, the control of piezoelectric actuators with multiple degrees of freedom (DOF) is not well settled. The main challenge in such system is the couplings between the different axis which should be considered during the control design since they may cause an unstability of the actuator [14][15]. This article addresses the motion control problem of a 2 degrees of freedom (DOF) piezoelectric cantilevered actuator (piezocantilever) by means of an embedded magnetic-based position sensors. While Hall effect is proposed as a basis for the displacement sensors, which permits high embeddability at low cost, a H_∞ control is proposed for the control in order to maintain a performances robustness.

In closed-loop, the position of the cantilever must be measured. This can be done with several sensing approaches. Non-contact external sensors can be used. very high resolution is not critical, these sensors are usually based on distance measurement with laser-based approaches [8], [16] or with confocal chromatic-based approaches [17], [18], [19]. Measurements based on the observation of periodic silicium nano-patterns with optical microscopy [20] are also possible when large displacements have to be measured with high resolution. If very high resolution is mandatory, interferometers have to be implemented [21], [22]. In vacuum environnement, electronic vision based on a Scanning Electron Microscope (SEM) is also a way to estimate displacements for nanorobotics tasks [23], [24]. The main drawback of external sensors is the size, which is significantly big compared with the micro-actuator, this fact prevents the implementation/design of compact and/or embedded control systems. The difficulty increases for applications that require multi-axial measurements. In order to overcome such limitation, sensors are integrated micro-actuators must be implemented (e.g. capacitive sensors) [25], [26].

[1]J. Escareno is with the Polytechnic Institute of Advanced Sciences, 7-9 rue M. Grandcoing, 94200 Ivry-sur-Seine, France

[2] AS2M department, FEMTO-ST Institute, UFC-CNRS-ENSMM-UTBM, Besançon, FRANCE

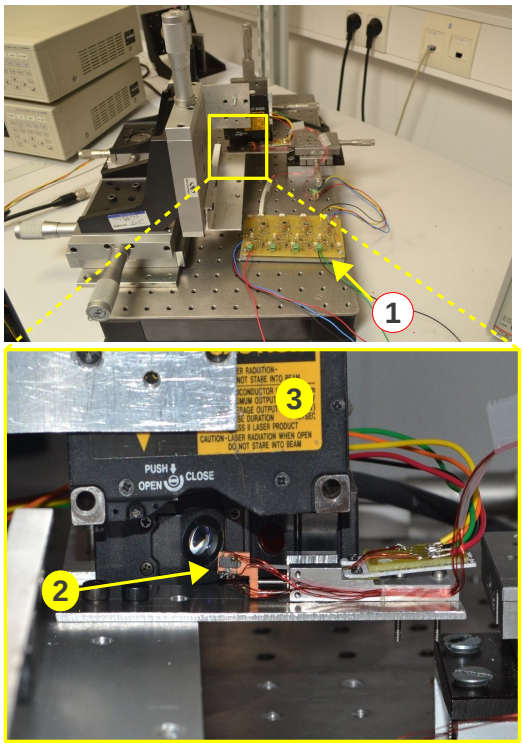

Fig. 1. Experimental setup: (1) Sensor's conditioning circuit, (2) Hall-effect sensors and (3) Keyence sensors.

Nevertheless, the resulting microsystem architecture is generally complex and difficult to tune.

The novelty and contribution of the paper consists in the estimation measurement of the piezocantilever tip displacement acquired *via* a magnetic-based sensing (MBS) system having embedded low-cost Hall-effect (HE) sensors. The results presented throughout the paper demonstrate that the MBS provide satisfactory performances for classical microrobotics applications. It is worth to highlight the MBS system's embeddability and low-cost. The MBS system is evaluated trough an application in robust control based on a H_∞ scheme. The experimental results show the effectiveness of the proposed sensing approach using low-cost magnetic sensors and H_∞ controller to regulate static and to track slow time-varying 2D reference signals.

The paper is organized as follows. In section-II, the experimental setup is presented. Section-III details the estimation approach used to obtain the actuator's displacements from the raw data provided by the magnetic sensors. While in the section-IV is presented the closed-loop control of the piezoelectric cantilever actuator using the H_∞ robust technique. Finally section-V provides concluding remarks and perspective works.

II. Experimental Setup

The experimental setup (Fig. 1) is composed of a 2-DOF piezocantilever, two embedded magnetic sensors (Fig. 2) and two external laser sensors which are used to validate the performances of the magnetic sensors. A dSPACE and computer real-time system is used to acquire the different signals and to implement the estimator and the controller. The piezoelectric cantilever actuator is based on 36 piezoelectric layers glued themselves which permit to work at low input voltage. This cantilever is controlled by two inputs U_y and U_z each one limited to ± 10 volts. One extremity of the cantilever is clamped while the other can bend in the 2D plane ($\vec{\delta}$) according to the input $\vec{U}$, as depicted on Fig.3 and such that:

$$\vec{\delta} = \begin{bmatrix} \delta_y \\ \delta_z \end{bmatrix} \qquad \vec{U} = \begin{bmatrix} U_y \\ U_z \end{bmatrix} \tag{1}$$

The scalar input U_y (resp. U_z) generates a displacement δ_y along axis y (resp. δ_z). However, unwanted displacement Z (resp. Y) due to the coupling is also observed. The behavior of the cantilever's displacement, yielded by the input $\vec{U}$, features couplings, hysteresis and creep [8].

The set of sensors used to perform the study are:

i) Two external laser sensors (LC2420 from *Keyence*) pointing at the tip of the piezocantilever in order displacement measurement along the y and z axes (see Fig. 1-Fig. 3). The Keyence sensors provide the measurement of $\vec{\delta}$, denoted as $\vec{L}_m$. They have $10nm$ resolution, $100\mu m$ to $200\mu m$ of precision and more than $1kHz$ bandwidth.

ii) Two hall-effect (HE) sensors (Micronas HAL401) embedded in the piezoelectric cantilever are used to

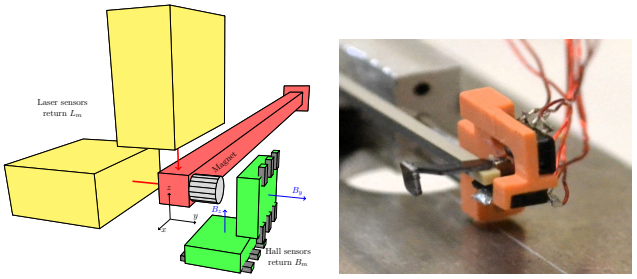

(a) CAD scheme.

(b) Photography of the magnetic sensors.

Fig. 2. Magnetic-based sensing system elements: piezoelectric cantilever actuator, hall-effect sensors (dimension: 4.5x2.5x1.2 mm^3) and magnet (dimension:1x1x1 mm^3)

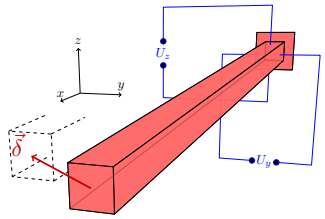

Fig. 3. Y-Z displacement of the piezoelectric actuator (dimension: 25x1x1 mm^3).

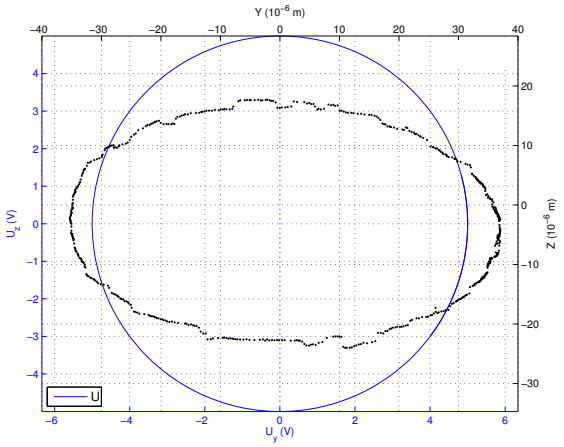

Fig. 4. Open loop response of the cantilever to a circular input U of frequency 0.1 Hz.

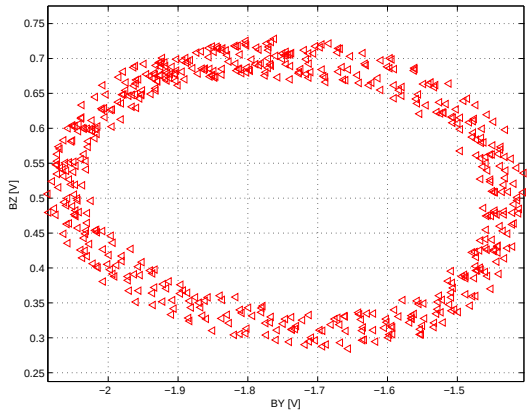

Fig. 5. Response B_m of the hall sensors to a circular input U of frequency 0.1 Hz.

acquire the magnetic field. Such sensors are orthogonally arranged in order to measure the magnetic field vector $\vec{B}_m$ arising from the 2D displacement of a magnet attached to the piezocantilever's tip (Fig. 2). The distance between this magnet and the HE sensors is therefore an image of the actuator's deflections. An estimated displacement $\hat{\vec{\delta}}$ is computed through an analytic function $f(\vec{B}_m)$, described in section III, such that:

$$\hat{\delta} = \begin{bmatrix} \hat{\delta}_y \\ \hat{\delta}_z \end{bmatrix} = f(B_m) \text{ with } \vec{B}_m = \begin{bmatrix} B_y \\ B_z \end{bmatrix} \quad (2)$$

The measurement of $\vec{L}_m$ and $\vec{B}_m$ are simultaneously obtained by a dSpace DS1005 acquisition system. The measurements performed by the Keyence sensors will be considered as reference measurements, which means that they are supposed to be the representation of the actual piezocantilever deflections, called position or displacement in this paper. This assumption leads to:

$$\vec{L}_m = \vec{\delta} \quad (3)$$

The characterization in open-loop of the piezoelectric actuator is shown in Fig. 4 and in Fig. 5. The characterization consists in applying a circular (U_y, U_z) inputs (using sinusoidal and cosinusoidal signals) of frequency equal to $0.1Hz$, corresponding to the blue solid-line in Fig. 4, while the black dot-line of Fig. 4 corresponds to the actual actuator displacement. One can notice the influence of the nonlinearities (hysteresis and creep) and the couplings arising from the simultaneous motion of the cantilever. Fig. 5 shows that magnetic field $\vec{B}_m$, resulting from the actuator's motion, follows a proportional behavior.

III. Estimation of the Piezocantilever's Displacements from Magnetic Field

The magnetic field $\vec{B}_m$ measured by the HE sensors is a function of the cantilever position $\vec{\delta}$:

$$\vec{B}_m = f'(\vec{\delta}) \quad (4)$$

This can be written as a system of two equations:

$$\begin{aligned} B_y &= g(\delta_y, \delta_z) \\ B_z &= h(\delta_y, \delta_z) \end{aligned} \quad (5)$$

where $g(\delta_y, \delta_z)$ and $h(\delta_y, \delta_z)$ are functions described later. In [30] and [29], Bancel and Ravaud propose a three dimensional analytical expression to compute the magnetic field $\vec{B}$ generated by a magnet. Such method provides an accurate estimation of $\vec{B}$ but the main drawback is that the expressions can not be analytically inverted. In our case, in order to retrieve the position of the magnet, the equations system Equ.5 is inverted such that:

$$\begin{aligned} \hat{\delta}_y &= g'(B_y, B_z) \\ \hat{\delta}_z &= h'(B_y, B_z) \end{aligned} \quad (6)$$

In order to simplify the analytic inversion, it is convenient to use simplified expressions for $g(\delta_y, \delta_z)$ and $h(\delta_y, \delta_z)$. We propose the following expressions:

$$\begin{aligned} B_y(\delta_y, \delta_z) &= A\delta_y + B\delta_z + C\delta_y\delta_z + D \\ B_z(\delta_y, \delta_z) &= E\delta_y + F\delta_z + G\delta_y\delta_z + H \end{aligned} \quad (7)$$

where A, B, ...,H are constant scalars to be numerically calculated during the calibration process of the HE sensors described in the next section. The inverted system giving the cantiveler position knowing the magnetic field measured by the HE sensors is:

$$\begin{aligned} \hat{\delta}_y(B_y, B_z) &= \frac{\alpha_1}{C\sqrt{\alpha_2}+\alpha_3} - \frac{B}{C} \\ \hat{\delta}_z(B_y, B_z) &= \frac{\sqrt{\alpha_4}+\alpha_5}{2(B.G-C.F)} \end{aligned} \quad (8)$$

with

$$\alpha_1 = B^2.E + C(B.\boldsymbol{B_z} - 2\,\boldsymbol{B_y}.F - B.H + 2\,D.F) - B(\boldsymbol{B_z}.C - C.H - \tfrac{2\,A.B.G}{C} + A.F + B.E - \boldsymbol{B_y}.G + D.G) - A.B.F + B.\boldsymbol{B_y}.G - B.D.G$$

$$\alpha_2 = (\boldsymbol{B_z}.C - A.F + B.E - \boldsymbol{B_y}.G - C.H + D.G)^2 - (4\,B.G - 4\,C.F).(A.\boldsymbol{B_z} - \boldsymbol{B_y}.E - A.H + D.E)$$

$$\alpha_3 = -\boldsymbol{B_z}.C^2 + C^2.H + 2\,A.B.G - A.C.F - B.C.E + \boldsymbol{B_y}.C.G - C.D.G$$

and

$$\alpha_4 = (\boldsymbol{B_z}.C - A.F + B.E - \boldsymbol{B_y}.G - C.H + D.G)^2 - 4(B.G - C.F)(A.\boldsymbol{B_z} - \boldsymbol{B_y}.E - A.H + D.E)$$

$$\alpha_5 = -\boldsymbol{B_z}.C + A.F - B.E + \boldsymbol{B_y}.G + C.H - D.G$$

A. Calibration of the Magnetic Sensor

The system described by Equ.8 requires a prior calibration before implementation. The calibration process consists in determining the scalar coefficients A, B, ...,H. The input is defined so that the cantilever's position follows a parametrized coordinates pattern covering the entire working space (Fig. 7). The frequency of the reference coordinates is low in order to avoid dynamic errors in the calibration. Then, the experimental displacement data δ_y, δ_z, B_y and B_z are acquired using the Keyence laser sensors and the HE sensors. The mean value of a 20 data set is computed for coordinate point of the pattern reducing the measurement noise in δ_y, δ_z, B_y and B_z. In order to obtain the function relating magnetic field and position it is applied a nonlinear least-squares curve fitting using the equations system Equ. 7 and the actual measured magnetic field. Fig. 6 shows the magnetic field from the identified parameters and Equ. 7 compared with its experimental measurement. This validates the calibration of the magnetic sensors. Having the parameters of Equ. 7, the inverse model (estimator) described by Equ.8 is yielded. Hence, the estimate displacements $\hat{\delta}_y$ and $\hat{\delta}_z$ are now available.

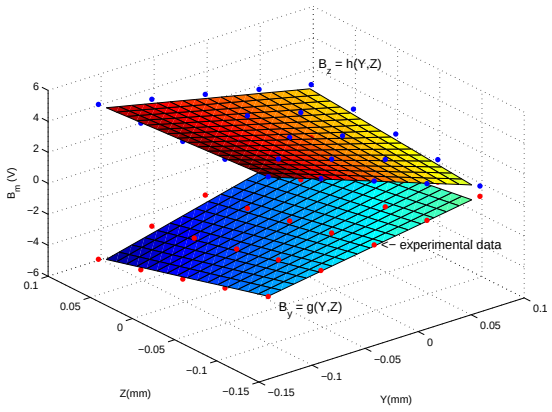

Fig. 6. Analytical estimation of the measured magnetic field B_m on the entire working space of the cantilever.

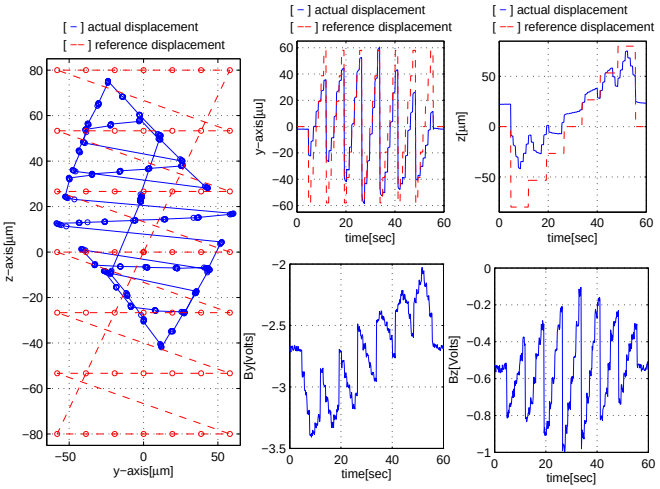

Fig. 7. Parametrized motion pattern to calibrate/estimate the cantilever displacement based on the magnetic field B_m throughout the entire working space.

IV. H_∞-based Control of the Piezo-cantilever

In this section, we use the estimate measurement $\hat{\delta}_y$ and $\hat{\delta}_z$ in a feedback control application. The H_∞ control technique is used for that. This permits to maintain the stability of the actuator and to improve its performances although the presence of the couplings and the nonlinearities (hysteresis and creep). The hysteresis nonlinearity yields uncertainties on the approximate linear model while the creep nonlinearity and the couplings can be considered as disturbances (see for instance [31]).

A. Model of the 2-DOF actuator

Assuming that the output displacements of the actuator is now available (thanks to the magnetic sensors), the 2-DOF piezoelectric actuator behavior can be described as follows [31]:

$$\begin{aligned} \delta_y &= k_y D_y(s) U_y + b_y = G_y(s) U_y + b_y \\ \delta_z &= k_z D_z(s) U_z + b_z = G_z(s) U_z + b_z \end{aligned} \tag{9}$$

where k_i is the static gain, $D_i(s)$ (such as $D_i(s=0) = 1$) is the dynamics and b_i is the disturbance, such that $i \in \{y, z\}$. Due to the hysteresis, the gain k_i (decribed in μm) is subjected to uncertainties. The disturbance b_i includes the creep, the couplings and a part of the hysteresis also. More details on their characterization can be found in [31]. The identification shows that:

$$G_y(s) = \frac{-0.4329(s-6863)(s-30)(s^2+1.19s+4.96\times10^7)}{(s+2913)(s+27)(s^2+457s+1.5\times10^7)}$$

$$G_z(s) = \frac{1.78(s+6838)(s+39)(s^2-3304s+2.17\times10^7)}{(s+1063)(s+35)(s^2+92s+1.5\times10^7)} \tag{10}$$

B. Standard H_∞ robust control

According to the model in Equ.9, we have two linear models each one with an with external disturbance. In this section, we calculate two controllers $C_y(s)$ and $C_z(s)$ for these two systems based on the standard H_∞ technique. With this technique, it is possible to *a priori* account these disturbances such that performances will still be maintained in their presence (performances robustness). The calculation of the two controllers is done with the same way. Hence, to ease the reading, let us denote $C(s)$ any of the controllers $C_y(s)$ and $C_z(s)$ and $G(s) = kD(s)U$ any of the systems $G_y(s)$ and $G_z(s)$. Fig. 8 pictures the block diagram of the closed-loop in which δ^r indicates the desired displacement.

1) Definition of the Specifications: The following specifications will be used for the calculation of the controller.

- *Tracking performances specifications:*
  For any of the displacements δ_y and δ_z, i.e. for δ of Fig. 8, we impose the following requirements:
  - a settling time no more than $30ms$,
  - zero overshoot,
  - and a statical error less than 1%.
- *Disturbance rejection:*
  It is wanted that the maximal error due to the disturbance b remain less than 2%.
- *Command moderation:*
  Finally, we also introduce a limitation of the input control U (i.e. U_y and U_z) such that it does not exceed $\pm 10V$ for the operating range of δ_r. This operating range is set equal to $\pm 35\mu m$ for the Y-axis and $\pm 25\mu m$ for the Z-axis. In fact, these values are taken from Fig. 4 which provided the output displacements when applying inputs of $\pm 10V$.

2) Standard form and standard H_∞ problem: From the above specifications, three weighting functions denoted $\mathcal{W}_1$, $\mathcal{W}_2$ and $\mathcal{W}_3$ are systematically introduced: the first one is intended to weight the error signal $\varepsilon(s)$ in order to account the tracking performances, the second is to account the command moderation and the third one is to weight the input disturbance signal $\vec{b}$ in order to account its rejection specifications.

Fig. 9 pictures the corresponding weighted closed-loop in which O_1 is the weighted output error signal and O_2 stands for the weighted control output, while I is the new disturbance accounting the weighting function. From this scheme, the standard scheme used for the controller synthesis is derived as depicted on Fig. 10. It consists of the interconnection between an augmented system $\mathcal{P}$ and the controller $C(s)$ to be synthesized. The input of the interconnection are composed of the exogenous signals δ^r and I, while the output is composed of the weighted signals O_1 and O_2 .

The standard H_∞ problem consists in finding an optimal value $\gamma > 0$ and the controller $C(s)$ stabilizing the interconnection in Fig. 10 and guaranteeing the following inequality:

$$\left\| \mathcal{F}_l\left(\mathcal{P}(s), C(s)\right) \right\|_\infty < \gamma \tag{11}$$

where $\mathcal{F}_l\left(\mathcal{P}_\eta(s), C_\eta(s)\right)$ is the lower linear fractionnar transformation between $\mathcal{P}(s)$ and$C(s)$ defined here as follows:

$$\begin{pmatrix} O_1 \\ O_2 \end{pmatrix} = \mathcal{F}_l\left(\mathcal{P}(s), C(s)\right) \begin{pmatrix} \delta^r \\ I \end{pmatrix} \tag{12}$$

From Fig. 9, we have:

$$\begin{aligned} O_1 &= W_1 S\delta^r - W_1 S W_3 I \\ O_2 &= W_2 C\delta^r - W_2 W_3 S C I \end{aligned} \tag{13}$$

where $S_\eta = (I + GC)^{-1}$ is the sensitivity function.

Using (Inequa. 11) and (Equ. 13), the standard H_∞ problem becomes into finding $C(s)$ and an optimal value of γ such that:

$$\begin{cases} \|W_1 S\|_\infty < \gamma \\ \|W_1 W_3 S\|_\infty < \gamma \\ \|W_2 S C\|_\infty < \gamma \\ \|W_3 W_2 S C\|_\infty < \gamma \end{cases} \tag{14}$$

which is satisfied if we find a controller ensuring the following inequalities:

$$\begin{cases} |S| = \bar{\sigma}_S < \gamma \left| \frac{1}{W_1} \right| \\ |S| = \bar{\sigma}_S < \gamma \left| \frac{1}{W_1 W_3} \right| \\ |SC| = \bar{\sigma}_{SC} < \gamma \left| \frac{1}{W_2} \right| \\ |SC| = \bar{\sigma}_{SC} < \gamma \left| \frac{1}{W_2 W_3} \right| \end{cases} \tag{15}$$

where $\bar{\sigma}_S$ and $\bar{\sigma}_{SC}$ are the upper singular values of S and of SC respectively. To solve the problem in (Equ. 15), we use the Glover-Doyle algorithm which is based on the Riccati equations [27][28]. The transfers $\frac{1}{W_1}$, $\frac{1}{W_1 W_3}$ and $\frac{1}{W_2}$ are called gabarits or bounds and

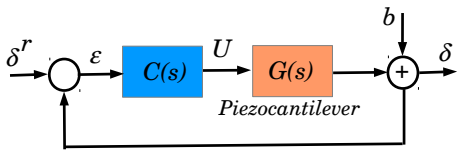

Fig. 8. The closed-loop system.

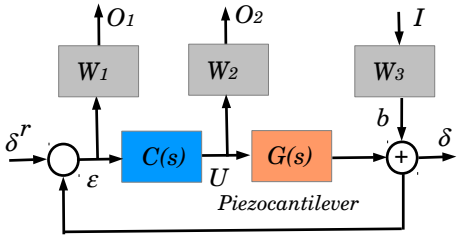

Fig. 9. Weighted closed loop system.

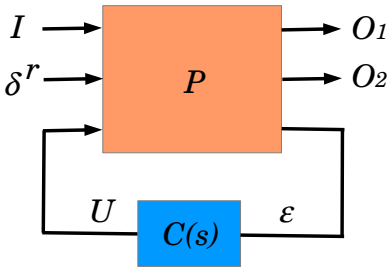

Fig. 10. The standard scheme showing exogenous inputs/outputs.

are calculated from the specifications in Section. IV-B as presented in the next subsection.

3) Derivation of the weighting functions: To obtain the weighting function $\frac{1}{W_1(s)}$, the specifications of tracking performances are used. To account the statical error ε_s, the settling time t_r and the no-overshoot transient part, we use the weighting function as follows:

$$\frac{1}{W_1} = \frac{K_{d_t} s + \frac{3}{\varepsilon_{s_t}}}{s + \frac{3}{t_{r_t}}} \tag{16}$$

where $t_{r_t} = 30ms$, $\varepsilon_{s_t} = 0.01$ and $k_{d_t} = 1$. Concerning the gabarit $\frac{1}{W_1 W_3}$, the disturbances rejection specifications are used. We use following gabarit for that:

$$\frac{1}{W_1 W_3} = \frac{K_{d_b} s + \frac{3}{\varepsilon_{s_b}}}{s + \frac{3}{t_{r_b}}} \tag{17}$$

where $t_{r_b} = 10ms$, $\varepsilon_{s_b} = 0.02$ and $k_{d_b} = 1$. Finally, the garabit corresponding to control moderation is written as

$$\frac{1}{W_2} = \frac{\delta_{max}}{U_{max}} \tag{18}$$

where $U_{max} = 10V$, and $\delta_{max} = 35\mu m$ for Y-axis and $\delta_{max} = 20\mu m$ for the Z-axis.

C. Experimental Results

The controllers $C_y(s)$ and $C_z(s)$ have been calculated. We obtained controllers order equal to 7. They have been implemented in Matlab-Simulink. A circular reference input has been applied to the closed-loop in order to check its efficiency to track complex trajectory at slow frequencies. Figures Fig. 11 and Fig. 12 depict the results obtained with a radius of $25\mu m$, and a frequency of 0.1Hz and 1Hz respectively. The figures show the reference to be tracked, the outputs from the magnetic sensors that are used for the feedback, and the actual outputs measured by the optical sensors. As we can see, the measurements from the used magnetic sensors well track the actual displacements. Furthermore, the closed-loop conveniently tracks the trajectory which demonstrates that the magnetic sensors can be successfully used for feedback applications. It is implicit that position regulation control is successfully assured. The experimental results demonstrate the viability of these proposed magnetic-based measuring sensors to deal with motion control of the 2-DOF piezocantilever.

V. CONCLUSION

The present paper has addressed the position control problem for a 2-DOF piezoelectric actuator using an alternative position sensing approach sensors based on magnetic field. To deal with such problem, we have implemented an embedded module using low-cost Hall-effect sensors and a magnet mounted on the actuator's tip. It is presented in detail the estimation-calibration process to obtain the position of the cantilever using the magnetic field row data. A H_∞ control algorithm is designed to

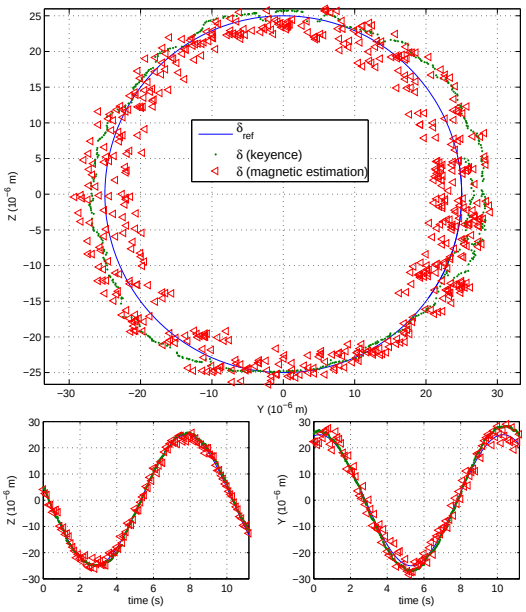

Fig. 11. Performance of cantiliver position control while tracking a circular reference at 0.1 Hz

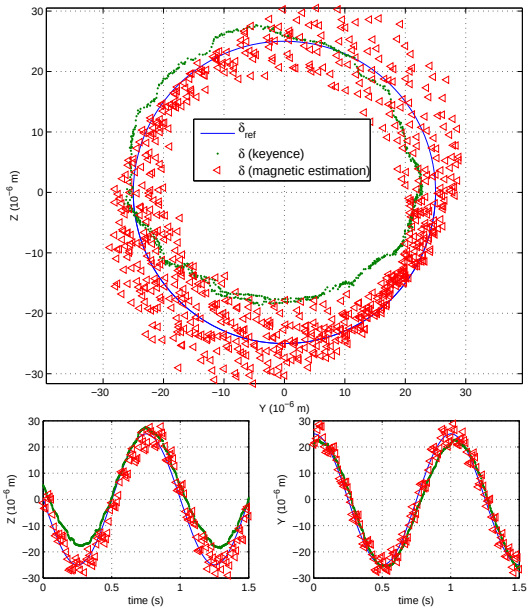

Fig. 12. Performance of cantiliver position control while tracking a circular reference at 1 Hz

overcome the non-linearities (creep, hysteresis and couplings) arising from the 2D motion of the piezocantilever. The proposed sensing approach results more attractive in terms of mechanical complexity in comparison with current position measurement techniques traduced in bulky and expensive sensors. The experimental results with closed-loop control of the actuator demonstrated the interest of the magnetic sensors in feedback applications.

ACKNOWLEDGMENT

This work was supported by the national ANR-Emergence MYMESYS-project (ANR-11-EMMA-006: High Performances Embedded Measurement Systems for multiDegrees of Freedom Microsystems), the CNRS-project MiM-HaC and the Equipex ROBOTEX project (contract "ANR-10-EQPX-44-01").

References

[1] F. Bancel and G. Lemarquand, "Three-dimensional analytical optimization of permanent magnets alternated structure," Magnetics, IEEE Trans on, vol. 34, no. 1, pp. 242-247, 1998.

[2] R. Ravaud and G. Lemarquand, "Magnetic field produced by a parallelepipedic magnet of various and uniform polarization," Progress In Electromag. Research, vol. 98, pp. 207-219, 2009.

[3] K. Kuhnen and H. Janocha, "Inverse feedforwrad controller for complex hysteretic nonlinearities in smart-materials systems", Control of Intelligent System, Vol.29, N^o3, 2001.

[4] B. Mokaberi and A. A. G. Requicha, "Compensation of scanner creep and hysteresis for AFM nanomanipulation", IEEE Transactions on Automation Science and Engineering, Vol.5, N^o2, pp.197-208, 2008.

[5] H. Jung, J.Y. Shim and D. Gweon, "New open-loop actuating method of piezoelectric actuators for removing hysteresis and creep", Review of Scientific Instr, 71 (9), pp.3436-3440, 2000.

[6] D. Croft, G. Shed and S. Devasia, "Creep, hysteresis and vibration compensation for piezoactuators: atomic force microscopy application", ASME Journal of Dynamic Systems, Measurement and Control, 2001.

[7] Micky Rakotondrabe, 'Bouc-Wen modeling and inverse multiplicative structure to compensate hysteresis nonlinearity in piezoelectric actuators', IEEE Trans on Autom Science and Engin, Vol.8(2), pp.428-431, April 2011.

[8] M. Rakotondrabe, C. Clevy, and P. Lutz, "Complete open loop control of hysteretic, creeped, and oscillating piezoelectric cantilevers," *IEEE Transactions on Automation Science and Engineering*, vol. 7, no. 3, pp. 440-450, 2010.

[9] M. Al Janaideh and P. Krejčí, "Inverse rate-dependent Prandtl-Ishlinskii model for feedforward compensation of hysteresis in a piezomicropositioning actuator," *IEEE/ASME Transactions on Mechatronics*, V.18(5), pp.1498-1507, 2013.

[10] K. K. Leang and S. Devasia, "Hysteresis, creep, and vibration compensation", IFAC Conference on Mechatronic Systems, pp.283-289, 2002.

[11] M. Rakotondrabe, Y. Haddab and P. Lutz, "Quadrilateral modeling and robust control of a nonlinear piezoelectric cantilever", IEEE Transactions on Control Systems Technology, Vol.17, Issue 3, pp:528-539, May 2009.

[12] S. Devasia, E. E. Eleftheriou, R. Moheimani, "A survey of control issues in nanopositioning", IEEE Transactions on Control Systems Technology, Vol.15, N^o15, pp.802-823, 2007.

[13] S. Khadraoui, M. Rakotondrabe and P. Lutz, 'Combining H-inf approach and interval tools to design a low order and robust controller for systems with parametric uncertainties: application to piezoelectric actuators', International Journal of Control (IJC), vol. 85, no1-3, pp. 251-259, 2012.

[14] M. Rakotondrabe, K. Rabenorosoa, J. Agnus and N. Chaillet, 'Robust feedforward-feedback control of a nonlinear and oscillating 2-dof piezocantilever', IEEE Transactions on Automation Science and Engineering, Vol.8(3), pp.506-519, 2011.

[15] Micky Rakotondrabe, Joël Agnus and Philippe Lutz, 'Feedforward and IMC-feedback control of a nonlinear 2-DOF piezoactuator dedicated to automated micropositioning tasks', IEEE - CASE, (International Conference on Automation Science and Engineering), pp.393-398, Trieste Italy, August 2011.

[16] Micky Rakotondrabe, Yassine Haddab and Philippe Lutz, "Nonlinear modeling and estimation of force in a piezoelectric cantilever", IEEE/ASME International Conference on Advanced Intelligent Mechatronics, pp. 1-6, 2007.

[17] Emmanuel Piat, Joël Abadie and Stéphane Oster, "Nanoforce estimation based on Kalman filtering and applied to a force sensor using diamagnetic levitation", Sensors and Actuators: A. Physical, Vol. 179, pp. 223-236, June 2012.

[18] Joël Abadie, Emmanuel Piat, Stéphane Oster and Mehdi Boukallel, "Modeling and experimentation of a passive low frequency nanoforce sensor based on diamagnetic levitation", Sensors and Actuators: A. Physical, vol.173, pp. 227-237, 2012.

[19] Ali Cherry, Emmanuel Piat and Joël Abadie, "Analysis of a passive microforce sensor based on magnetic springs and upthrust buoyancy", Sensors and Actuators : A. Physical, vol. 169, n°1, pp. 27-36, september 2011

[20] July Galeano Zea , Patrick Sandoz , Guillaume J. Laurent , Lucas Lopes Lemos and Cédric Clevy, "Twin-scale Vernier Micro-pattern for Visual Measurement of 1-D in-plane Absolute Displacements with Increased Range-to-Resolution Ratio", International Journal of Optomechatronics, volume 7, issue 3, pp. 222-234, 2013.

[21] Mokrane Boudaoud, Yassine Haddab, and Yann Le Gorrec, "Modeling and optimal force control of a nonlinear electrostatic microgripper". IEEE/ASME Transactions on mechatronics (T-Mech). Vol.18, Issue 3, pp. 1130-1139. June 2013.

[22] Mokrane Boudaoud, Yassine Haddab, Yann Le Gorrec and Philippe Lutz, "Noise characterization in millimeter sized micromanipulation systems". International journal of Mechatronics, IFAC vol 21, pp. 1087-1097, 2011.

[23] Naresh Marturi, Brahim Tamadazte, Sounkalo Dembélé and Nadine Piat, "Visual servoing-based approach for efficient autofocusing in scanning electron microscope", IEEE/RSJ Int. Conf. on Intelligent Robots and Systems, pp. 2677-2682, 2013.

[24] Christian Dahmen and Sergej Fatikow, "Tracking of objects in motion-distorted scanning electron microscope images", IEEE/RSJ Int. Conf on Intelligent Robots and Systems (IROS), pp. 19-24, 2011.

[25] E. T. Enikov and B. J. Nelson, "Three-dimensional microfabrication for a multi-degree-of-freedom capacitive force sensor using fibre-chip coupling", Journal of Micromechanics and Microengineering, Vol. 10, no. 4, 2000.

[26] S. Muntwyler, F. Beyeler and B. J. Nelson, "Three-axis microforce sensor with tunable force range and sub-micronewton measurement uncertainty", IEEE Int. Conf. on Robotics and Automation (ICRA), pp. 3165 - 3170 , 2010.

[27] K. Glover and J. C. Doyle, "State-space formulae for all stabilizing controllers that satisfy an H_∞-norm bound and relations to risk sensivity", Systems & Control Letters, vol.11, pp.167-172, 1988.

[28] J. C. Doyle, K. Glover, P. K. Khargonekar and B. A. Francis, "Statespace solutions to standard H2 and H_∞ control problems", IEEE Transaction Automatic Control, AC 34 No8, pp.831-846, 1989.

[29] Ravaud, R. and Lemarquand, G., Magnetic field produced by a parallelepipedic magnet of various and uniform polarization Progress In Electromagnetics Research, 2009, 98, 207-219

[30] Bancel, F. and Lemarquand, G., Three-dimensional analytical optimization of permanent magnets alternated structure Magnetics, IEEE Transactions on, 1998, 34, 242-247

[31] Micky Rakotondrabe, 'Modeling and robust H-inf control of a nonlinear and oscillating 2-dof multimorph cantilevered piezoelectric actuator', a chapter in 'Smart materials-based actuators at the micro/nano-scale: characterization, control and applications' edited by Micky Rakotondrabe, Springer - Verlag, New York, ISBN 978-1-4614-6683-3, 2013.